Critical threshold for microtubule amplification through templated severing

Marco Saltini and Bela M. Mulder
AMOLF, Science Park 104, 1098XG Amsterdam, Netherlands

The cortical microtubule array of dark-grown hypocotyl cells of plant seedlings undergoes a striking, and developmentally significant, reorientation on exposure to light. This process is driven by the exponential amplification of a population of longitudinal microtubules, created by severing events localized at crossovers with the microtubules of the pre-existing transverse array. We present a dynamic one-dimensional model for microtubule amplification through this type of templated severing. We focus on the role of the probability of immediate stabilization-after-severing of the newly created lagging microtubule, observed to be a characteristic feature of the reorientation process. Employing stochastic simulations, we show that in the dynamic regime of unbounded microtubule growth, a finite value of this probability is not required for amplification to occur but does strongly influence the degree of amplification and hence the speed of the reorientation process. In contrast, in the regime of bounded microtubule growth, we show that amplification only occurs above a critical threshold. We construct an approximate analytical theory, based on *a priori* limiting the number of crossover events considered, which allows us to predict the observed critical value of the stabilization-after-severing probability with reasonable accuracy.

I. INTRODUCTION

Microtubules are a ubiquitous component of the cytoskeleton in eukaryotic cells. They are filamentous aggregates of tubulin dimers reaching lengths of several μm's. They are typically part of structures that span the dimensions of the whole cell, enabling, e.g., their major role in intracellular transport by providing "tracks" for cargo carrying motor proteins and cell division where they form the mitotic spindle responsible for the spatial segregation of the duplicated chromosomes [1]. The fact that during the cell cycle microtubules can be reassembled into different spatial structures is due to their intrinsically dynamic nature. They stochastically switch between phases of growth through polymerization to phases of shrinkage through rapid depolymerization, a mechanism that has been dubbed dynamic instability [2]. A direct consequence of this mechanism is that microtubules have a finite lifetime, as they can shrink away, and therefore need to be actively (re)nucleated to sustain their overall number. Cells achieve control over the microtubule structures they build by manipulating the nucleation and dynamics of microtubules in space and time, using specific nucleating complexes and a host of microtubule-interacting proteins (MAPS) [3].

Growing plant cells have a unique microtubule structure called the cortical array. The cortical array is an assembly of mutually aligned microtubules localized close to the cell membrane that almost homogeneously covers the inside surface of the cell. Generically the preferential direction of the cortical microtubules is transverse to the long axis of the cell. This is crucial to their function, as they guide the anisotropic deposition of cell-wall building polymers, which in turn allows the cell to grow along a single expansion axis. In this way the cortical array drives the dominant mode of morphogenesis in plants, which is the formation of linear extensions, like roots, stems and branches. However, it is known that this generic growth scenario can be modulated by hormonal, mechanical and other environmental signals [4]. A striking example of this type of modulation is the reorientation of the cortical array of dark-grown hypocotyl (stem precursor) cells after exposure to blue light [5]. This effect is highly relevant, as the developmental program of the plant must change dramatically, once the hypocotyl, which typically emerges from a buried seed, first reaches the sunlight. It is believed that the observed reorientation from the transverse to the longitudinal orientation of the cortical array is associated with the arrest of further growth, and the subsequent differentiation of the cells.

The light-induced reorientation of the cortical array is mediated by the microtubule severing protein *katanin*. It has been shown to localize at the crossover between differently oriented cortical microtubules and, moreover, to preferentially sever the overlying microtubule, i.e., the one that crossed over a pre-existing one. As the underlying microtubule is most likely to be a transversely oriented microtubule from the pre-exposure state and severing effectively multiplies the number of microtubules, this effect can rapidly create an exponentially growing population of longitudinal microtubules. In this way the original transverse cortical array serves as a template for the reorientation toward a longitudinal array.

Recent experiments involving a number of mutants in which the reorientation effect is impaired have shown that there is an important role for the propensity of the newly created plus end of the lagging microtubule to immediately switch to the growing state, a process which *in vivo* is mediated by the prominent MAP *CLASP* [6]. This specific function of *CLASP* appears to have evolved, as the default outcome of a severing event is the creation of a shrinking plus end of the lagging microtubule [7]. In particular, Lindeboom *et al.* [6] experimentally showed that the concentration of *CLASP* at severing sites is positively correlated with the

stabilization of the newly created plus end after severing and, therefore, with its immediate growth. Indeed, in higher plants, *CLASP* localizes not only at growing plus ends but also along the lattice of microtubules [8], where severing events take place. Furthermore, stochastic simulations of a simplified model of the reorientation mechanism, showed that the degree of amplification of the numbers of microtubules due to severing increases monotonically with the probability of the so-called stabilization-after-severing of the lagging plus end [6]. However, the dynamic parameters of the microtubules measured in the experiments suggest that, at least in the initial phase of reorientation, the microtubules are in the so-called unbounded-growth regime [9]. Since in this regime the microtubules in principle are very long lived on the timescale of the reorientation, this raises the question to what extent stabilization-after-severing is in fact a necessary ingredient of the mechanism. Unfortunately, as all microtubules experimentally studied were in the unbounded-growth regime, there are no data about the reorientation process in the bounded-growth regime. However, one can argue that, as the total amount of tubulin in the cell is finite, the unbounded-growth and amplification of microtubules cannot be sustained indefinitely, as the pool of available tubulin to drive polymerization is inevitably depleted. This would cause the growth speed of the microtubules to decrease, effectively driving them back to the bounded-growth regime. To fully understand the reorientation process we thus need to disentangle the role of the microtubule growth state from that of the probability of stabilization-after-severing, and this is the main aim of this paper. We approach this problem using a combination of stochastic simulations and analytical theory, which together allow us to fully characterize the requirements for the amplification of longitudinal microtubules to occur.

The structure of the paper is as follows. In Sec. II we introduce our dynamic model of longitudinal microtubules undergoing dynamic instability and severing in the presence of a grid of stable transverse microtubules. We then briefly review some of the main features of Dogterom-Leibler model for microtubules undergoing dynamic instability [9], on which our model is based. In Sec. III we show how, for microtubules in the unbounded-growth regime, while not a necessary ingredient, the probability of stabilization-after-severing does dramatically affect the speed and ultimate success probability of amplification of the longitudinal microtubule population. Then we extend our treatment to the bounded-growth regime, showing that in this case amplification can occur provided that the probability of stabilization-after-severing exceeds a critical threshold. Finally, we calculate the critical value for the probability of stabilization-after-severing using a combination of analytical calculations and computer simulations. To that end, we introduce an approximate theory in which each microtubule can experience at most two crossovers, allowing an analytical determination of the contribution of the probability of stabilization-after-severing to the probability that the creation of a crossover actually leads to a severing event and hence contributes to the amplification. In order to do so, we develop a novel approximate technique to calculate the first-passage time distribution (FPTD) for the microtubules to reach relatively close targets, which has potential application for studying first-passage time problems in other systems as well.

II. THE MODEL

A. Dynamic model

In order to better understand the importance of the probability of stabilization-after-severing for the reorganization mechanism of the cortical microtubule array, we introduce a stochastic model of longitudinal microtubules undergoing dynamic instability in a one dimensional grid of transverse microtubules. We limit our study of the system only to the first stage of the reorientation process, i.e., the first 500 s, for three distinct reasons. First, since prior to the exposure to light the transverse array consists of relatively long microtubules which would take significant time to depolymerize to a degree affecting our proposed mechanism, the array can in the initial stage of this process be regarded as a constant background structure, while for longer time periods it begins to "dissolve" due to ongoing depolymerization, and therefore its dynamics can no longer be ignored. Second, experiments have shown that, while the full reorientation of the microtubule array requires from 30 to 60 min to complete, the amplification of the number of longitudinal microtubules typically takes place in the first 10 min after the exposure to blue light [6]. Finally, given that our model produces an exponentially increasing number of microtubules (see Sec. III), running the required simulations for more than 500 s would be computationally too costly.

The model consists of a single longitudinal microtubule undergoing dynamic instability in the one dimensional grid of stable, transverse microtubules with constant spacing d between neighboring filaments [10]. According to experimental observations, where the angle between differently oriented microtubules is very close to $90°$, we assume that all longitudinal microtubules are exactly perpendicular to the transverse. The microtubule is nucleated at position $x = 0$ with plus end in the growing state with growing speed v^+, and it can switch to shrinking state with constant catastrophe rate r_c. Once it is in the shrinking state, either its plus end shrinks back to position $x = 0$ and dies, or it undergoes a rescue with constant rate r_r, switching back to the growing state.

Every time the plus end reaches a transverse microtubule, i.e., when its position is $x = nd$ with $n \in \mathbb{N}$, it creates a crossover. This crossover can be resolved in two distinct ways: either it is removed by the shrinkage of the microtubule due to its dynamic instability, or it survives long enough to lead to a severing event. Whether or not the severing event occurs is determined not only by the dynamic instability of the longitudinal microtubule, but also by an intrinsic severing waiting time distribution at the crossover that can be, in principle, arbitrary. This distribution accounts for the fact that *katanin* requires a certain amount of time to localize at crossovers and be properly assembled before being able to sever microtubules. We choose this severing waiting time distribution to be of the form

$$W_{k,\theta}(t) = \frac{t^{k-1}}{\theta^k \Gamma(k)} e^{-\frac{t}{\theta}}, \qquad (1)$$

i.e., the gamma probability density function [11], where

$$\gamma(k) = \int_0^\infty ds\, s^{k-1} e^{-s}, \qquad (2)$$
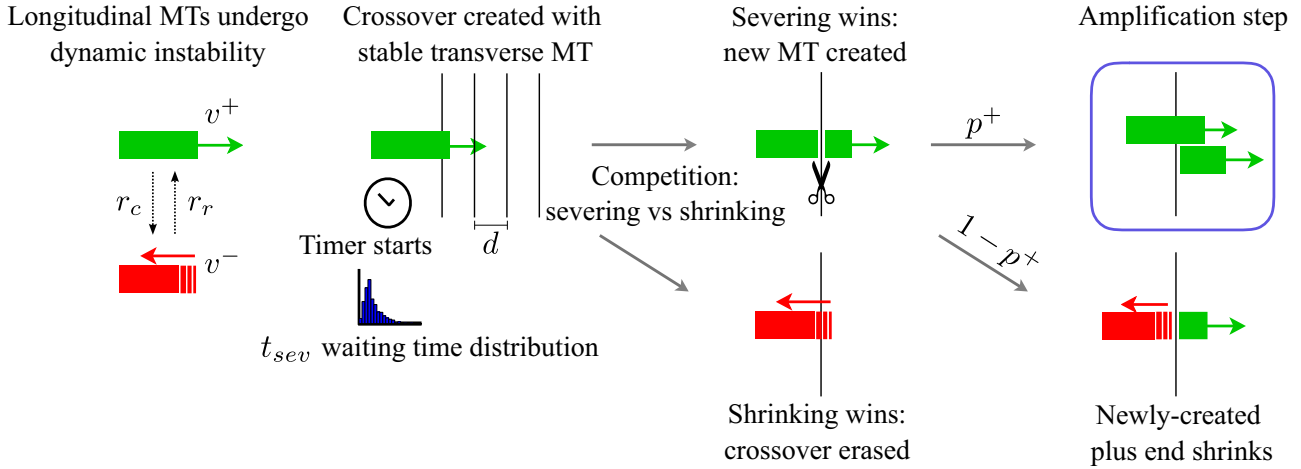
FIG. 1. Schematic of the model of longitudinal microtubules undergoing dynamic instability in a grid of stable transverse microtubules. After a crossover creation, a competition between the intrinsic severing waiting time and crossover removal due to dynamic instability takes place. If severing occurs, then the newly created plus end is rescued with probability p^+.

is the Euler gamma function, k is the shape, and θ is the scale parameter of the distribution. We adopted the value $k = 7$, as this value was shown to provide a good fit to the experimentally measured severing waiting time distribution [6]. However, we stress that the choice for a specific form of the distribution is a pragmatic one, and in the absence of further insight into the details of the molecular processes that lead up to a severing, we cannot speculate whether this, e.g., is in fact evidence for an underlying seven-step Poisson process, which potentially could explain the specific form of the distribution (1). This would require further investigations aimed at understanding the full mechanism of the severing process driven by *katanin*.

When a severing event occurs, the former long microtubule is split in two shorter microtubules, both of them keep undergoing dynamic instability and can create new crossovers and being severed again, in order to amplify the number of longitudinal microtubules. Hereafter, we adopt the convention of calling the "lagging" microtubule as being the newly created one, while the "leading" microtubule, with the unperturbed original plus-end as the original one, consistent with the fact that the severing events increases the number of microtubules by 1. The newly created plus end of the lagging microtubule either is stabilized and it enters the growing state with probability p^+, or it enters the shrinking state with probability $1 - p^+$. The newly created minus end of the leading microtubule is now positioned at the severing point and in a stable state, consistent with the experimental observation that the stability of microtubule minus end is promoted by the presence of *SPIRAL2* protein, which tracks the minus end of microtubules and prevent them from subunit loss [10], while no changes are applied to its plus end, see Fig. 1.

B. Microtubule behavior in the interstitial strip

After the creation of a crossover and before the creation of a second one, the dynamics of the plus end of a microtubule is described by the Dogterom-Leibler model for microtubules undergoing dynamic instability [9]. We are aware that several

effects in microtubule dynamics have been reported that go beyond this widely adopted basic model, such as a time-dependent increase in catastrophe rate due to microtubule ageing (see, e.g., Ref. [12] as well as a time-dependent increase in rescue rate due to microtubule healing (see, e.g., Ref. [13]), we posit that these effects are secondary in nature, and as such beyond the scope of the present model, which aims at establishing basic principles. Notice that the dynamics of the plus end is not influenced by eventual severing events. Therefore, as long as the plus end is at $x \in (nd, (n+1)d)$, we can study the property of the correspondent microtubule undergoing dynamic instability in a strip of width d as if its length is $l = x - nd$.

In the non-confined-in-a-strip case, the model has two possible solutions for the probability distribution of microtubule length: in the bounded-growth regime, defined by the relation $\bar{l} > 0$, with

$$\bar{l} = \left(\frac{r_c}{v^+} - \frac{r_r}{v^-} \right)^{-1}, \tag{3}$$

the steady-state solution is reached, and the length distribution is an exponential decay proportional to $e^{-l/\bar{l}}$, while in the unbounded-growth regime the average length of microtubules grows linearly in time, with the length distribution that is well approximated by a Gaussian-like function [9].

When microtubule dynamics is confined in a strip of a finite width, however, both the bounded and the unbounded-growth regimes lead to a steady-state solution for the length distribution that is proportional to $e^{-l/\bar{l}}$. Notice that, in the unbounded-growth regime case, $\bar{l}$ is no longer positive, and hence the distribution is exponentially increasing [14]. General features regarding the lifetime distribution and the splitting probabilities of microtubules in the Dogterom-Leibler model can be found in Appendix A.

Given our specific interest in studying the properties of the system in both the bounded and the unbounded-growth regime, we have chosen two sets of dynamic parameters: For the bounded-growth case parameters are chosen accordingly to previous observations [15], while for the

TABLE I. Model parameters.

Parameter	Description	Numerical value (bounded-growth)	Numerical value (unbounded-growth)	Units
v^+	Growth speed	0.1	0.103	$\mu\mathrm{m\,s^{-1}}$
v^-	Shrinkage speed	0.25	0.225	$\mu\mathrm{m\,s^{-1}}$
r_c	Catastrophe rate	0.02	0.0058	$\mathrm{s^{-1}}$
r_r	Rescue rate	0.02	0.026	$\mathrm{s^{-1}}$
p^+	Probability of stabilization-after-severing	Tuned	Tuned	—
d	Spacing between neighbors	1.5	1.5	$\mu\mathrm{m}$
θ	Scale parameter of Γ distribution	8.5	8.5	s
k	Shape parameter of Γ distribution	7	7	—

unbounded-growth case, both dynamic parameters and grid parameters are those that have been directly measured for the WT case by previous experimental works [6], see Table I.

III. RESULTS

A. Amplification in the unbounded-growth regime

We already partially studied the model introduced in Sec. II computationally for microtubules in the unbounded-growth regime in earlier work [6]. There, the model was used to show that the major contribution to the speed of amplification of longitudinal microtubules was the probability of stabilization-after-severing p^+ rather than the intrinsic rescue rate r_r of microtubules.

Here we perform an in-depth study of the response to the system to the change of p^+. We will show that in the unbounded-growth regime, although the value of p^+ is indeed crucial for determining the *speed* of amplification, a nonzero value of p^+ is in fact *not* required for amplification to occur. This seemingly counterintuitive result will be explained later in terms of the dynamic properties of the unbounded-growth regime.

Our simulations consist of $N = 10^5$ trials in which a single longitudinal microtubule undergoes dynamic instability in the whole grid of transverse microtubules. For every trial we keep track of the fate of the initial microtubule and its offspring until either no more microtubules are present, i.e., they all have shrunk to length zero, and we call this possible output extinction, or, for every trial that did not result in an extinction, the number of microtubules is exponentially increasing, and we call this second possible output amplification.

Figure 2(a) shows that for our choice of dynamic parameters, the speed of amplification increases with p^+. Furthermore, we notice from Fig. 2(b) that greater values of p^+ correspond to lower extinction probabilities, suggesting that a good stabilization-after-severing entails a double effect: It not only increases the speed of amplification but also makes the amplification occur more likely.

The interesting result that in the unbounded-growth regime even the $p^+ = 0$ case leads to an overall amplification can be explained by an intrinsic property of the regime itself. Indeed, although every severing event shortens the length of the severed microtubule, its plus end is not affected by such an event. Consequently, the dynamic properties of the leading microtubule are not changed by the severing, and so it applies to the microtubule lifetime as well. Since, on average,

the length of microtubules in the unbounded-growth regime grows as

$$J = \frac{r_r v^+ - r_c v^-}{r_r + r_c} t, \tag{4}$$

it follows that the average lifetime of microtubules is infinite [9], and therefore there is no upper bound for the number of severing events that a microtubule can undergo. Indeed, a shrinking microtubule in this regime always has a finite probability to switch back from the shrinking to the growing state, and fully recover any amount of lost length, regardless of p^+.

B. Amplification in the bounded-growth regime

In this section, we address the question whether the amplification occurs regardless of p^+ in the bounded-growth regime as well as in the unbounded-growth case. To do so we perform computer simulations for microtubules in the bounded-growth regime (see Table I) to show that p^+ needs to be greater that a certain critical value p_{crit}^+ in order have amplification. Moreover, using a combination of computer simulations and analytical calculations we identify such a critical value as a function of the other model parameters.

1. Critical point in simulations

By tuning the probability of stabilization-after-severing p^+ from 0 to 1, we observe two different behaviors, see Fig. 3(a): For lower values of p^+ the average number of microtubules exponentially decays in time (extinction), while for higher values of p^+ the number of microtubules exponentially increases (amplification). It follows that there exists a critical threshold for p^+ above which the average output is amplification. For our choice of model parameters, the computationally measured critical value is $p_{\mathrm{crit}}^+ \simeq 0.36$. Therefore, if we define the *amplification probability* as the fraction of trials the output of which is amplification, then we observe that below the critical threshold the amplification probability is zero, while it is greater than zero otherwise, see Fig. 3(b).

2. Calculation of the critical point

When microtubule is created through a severing event, either it shrinks to length zero and dies or it is severed a sufficient number of times to create an offspring of new lagging microtubules. If the size of such an offspring is, on
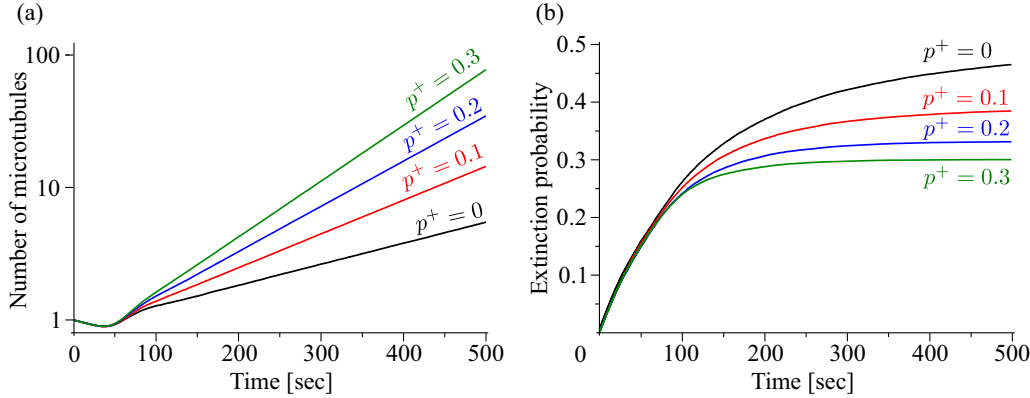
FIG. 2. (a) Time evolution of the number of longitudinal microtubules for four different values of p^+. They all exhibit amplification. (b) Extinction probability as a function of time. It represents the fraction of trials in which, after a certain amount of time, all microtubules have completely depolymerized. Results are averaged over $N = 10^5$ simulation.

average, greater than 1, then the output is amplification. In other words, if M is the number of severing events that a newly created microtubule undergoes, then amplification occurs if, on average,

$$M > 1. \tag{5}$$

To fix the ideas, suppose that a microtubule is created by severing with initial length $x = d$. Then, with probability p^+, it is initially created in the growing state and consequently with probability $1 - p^+$ in the shrinking state. It follows that the size of the offspring of the mother microtubule can be written as $M = p^+ M^+ + (1 - p^+)M^-$, where M^σ is the size of the offspring of a microtubule created in the state σ. However, since a shrinking microtubule with plus end at $x < d$ cannot be severed, M^- equals M^+ times the probability that the shrinking microtubule recovers the length at birth d, i.e., $M^- = R_d^-(d)M^+$, where $R_d^-(d)$ is the splitting probability defined in the Appendix A. Hence, the condition expressed in Eq. (5) can be rewritten as

$$M = [p^+ + (1 - p^+)R_d^-(d)]M^+ > 1. \tag{6}$$

By solving the equality related to Eq. (6) we can find the critical value of $p^+ = p_{\text{crit}}^+$ above which amplification takes place

$$p_{\text{crit}}^+ = \frac{1 - R_d^-(d)M^+}{(1 - R_d^-(d))M^+}. \tag{7}$$

As p_{crit}^+ can only take allowed values between 0 and 1, depending on M^+ and $R_d^-(d)$, situations exist in which amplification cannot occur and others in which it always occurs. Indeed, from Eq. (7), we immediately see that if $M^+ < 1$ then $p_{\text{crit}}^+ > 1$, i.e., if the average size of the offspring of mother microtubules born in growing state is smaller than 1, amplification is impossible. On the other hand, if $M^+ R_d^-(d) > 1$, or $M^- > 1$, then it follows that $p_{\text{crit}}^+ < 0$, i.e., if the average size of the offspring of mother microtubules born in the shrinking state is greater than 1, then amplification always occurs.

It is important to underline that, in our discussion, we assumed that all microtubules were born with initial length d. This choice implies that all severing events occur at the first crossover. However, given the stochastic nature of the system and of the severing waiting time probability of Eq. (1), it is possible that a severing event occurs further in the grid than at the first crossover of a microtubule. In other words, the initial length of a newly created microtubule can be $x = nd$, with $n > 1$.
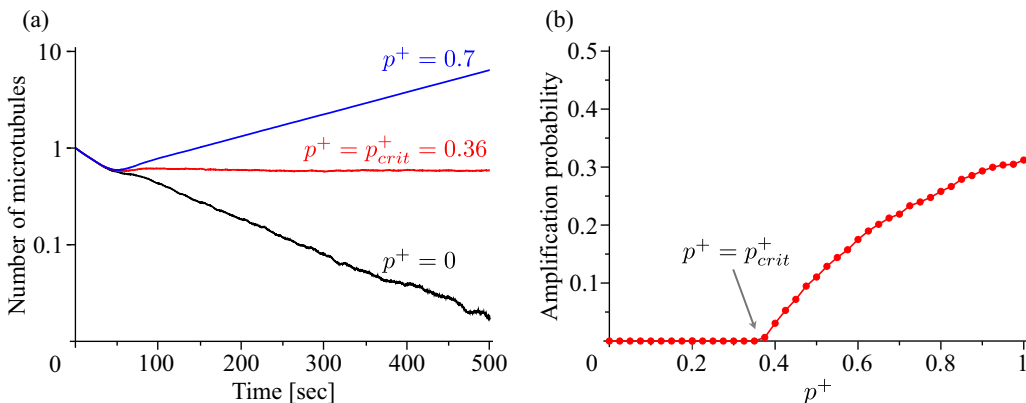
FIG. 3. (a) Time evolution of the number of longitudinal microtubules for three different values of p^+. One leads to amplification (blue line), one to extinction (black line), and one corresponds to the critical behavior (red line). (b) Amplification probability as a function of p^+. Amplification probability is nonzero for p^+ larger than $p_{\text{crit}}^+ \simeq 0.36$. Results are averaged over $N = 10^5$ simulation.

TABLE II. Comparison p_{crit}^+ vs. $p_{\mathrm{crit},(1)}$ vs. $p_{\mathrm{crit},(2)}$ for different sets of dynamic parameters as v^+, v^-, r_c, and r_r. All other model parameters are those of Table I. $\Delta p_{(1)}^+ = \frac{p_{\mathrm{crit}}^+ - p_{\mathrm{crit},(1)}^+}{p_{\mathrm{crit}}^+}$ and $\Delta p_{(2)}^+ = \frac{p_{\mathrm{crit}}^+ - p_{\mathrm{crit},(2)}^+}{p_{\mathrm{crit}}^+}$ represent the relative error of the one and two-crossovers theory to the computationally measured critical value for the probability of stabilization-after-severing.

Dynamic parameters				Simulations	1-cross. approximation		2-cross. approximation	
				Critical point	Critical point	Relative error	Critical point	Relative error
v^+ (μm s^{-1})	v^- (μm s^{-1})	r_c (s^{-1})	r_r (s^{-1})	p_{crit}^+ —	$p_{\mathrm{crit},(1)}^+$ —	$\Delta p_{(1)}^+$ —	$p_{\mathrm{crit},(2)}^+$ —	$\Delta p_{(2)}^+$ —
0.10	0.250	0.020	0.020	0.360	0.316	0.122	0.361	0.003
0.08	0.275	0.016	0.022	0.338	0.297	0.121	0.337	0.003
0.15	0.225	0.020	0.020	0.142	0.108	0.239	0.144	0.014
0.10	0.250	0.030	0.015	0.882	0.819	0.071	0.864	0.020
0.10	0.250	0.015	0.030	0.089	0.068	0.236	0.103	0.157
0.10	0.250	0.030	0.015	0.800	0.733	0.084	0.780	0.025
0.10	0.275	0.020	0.030	0.285	0.240	0.158	0.285	0.000
0.10	0.250	0.010	0.020	0.054	0.041	0.241	0.066	0.222
0.08	0.225	0.015	0.025	0.208	0.179	0.139	0.213	0.024
0.12	0.225	0.020	0.025	0.175	0.140	0.200	0.179	0.023
0.08	0.250	0.002	0.020	0.510	0.455	0.108	0.497	0.025

In this case, we need to add into the count of the size of offspring of a mother microtubule all cases in which a microtubule that is born with initial length nd, $n > 1$, it is also severed at $(n-1)d$, $(n-2)d$, ... We consider the microtubules created by this mechanism as direct daughter microtubules of the mother microtubule we are measuring the size of the offspring of. To that end, we first define m_i via $M^+ = \frac{1}{N} \sum_{i=1}^{N} m_i$ as the number of microtubules generated by the mother microtubule labeled by i, and N is the number of microtubules we keep track of the fate. Then, we denote the number of severing events the microtubule i undergoes with s_i, and the position of the crossover at which the first severing takes place with c_{j_i}, with the rule: $c_{j_i} = n - 1$ if the severing occurred at nd. Since after a severing event at nd the crossovers at kd, $k < n$, can be removed by either shrinkage or severing, we define $b_{c_{j_i}}$ as the number of crossovers that are resolved by shrinkage. Therefore

$$m_i = s_i + \sum_{j_i=1}^{s_i} \left[c_{j_i} - b_{c_{j_i}} \right]. \tag{8}$$

Notice that $b_{c_{j_i}}$ depends on p^+, as it depends on the behavior of the plus end after severing of the newly created microtubule. Consequently, the right-hand side of Eq. (7) exhibits a dependency on p^+. Hence, we need to find the exact dependency on p^+ of $b_{c_{j_i}}$. To avoid the problem, in first approximation we set $b_{c_{j_i}} = 0$ for every c_{j_i}. In this way, we can computationally measure $m_i^{(1)} \equiv s_i + \sum_{j_i=1}^{s_i} c_{j_i}$, and we use Eq. (7) to give a first estimate of the critical probability $p_{\mathrm{crit},(1)}^+$, see Table II. We refer to this approximation as *one-crossover* approximation. From the table we notice that, although this approximation gives a reasonable prediction for the critical probability of stabilization-after-severing, it systematically underestimates it.

Analytically, one can calculate $b_{c_{j_i}}$ only under the condition that a severing event at nd always implies the resolution of the crossovers at d, $2d$, ..., $(n-2)d$ through a severing event, while the crossover at $(n-1)d$ can be resolved by either severing or shrinkage. Therefore, if we denote the probability of resolving this crossover with a shrinkage as $p_{\mathrm{cr}}(p^+)$, we have

$$b_{c_{j_i}} = \left(1 - \delta_{c_{j_i},0}\right) p_{\mathrm{cr}}(p^+). \tag{9}$$

The Kronecker function $\delta_{c_{j_i},0}$ of Eq. (9) accounts the fact that if the severing happens at d (i.e., $c_{j_i} = 0$), then no other crossovers are removed by either severing or shrinkage. If we plug Eq. (9) into Eq. (8), then we can now calculate an approximate expression for M^+, i.e.,

$$
\begin{aligned}
M_{(2)}^+ &= \frac{1}{N} \sum_{i=1}^{N} m_i^{(2)} \\
&= \frac{1}{N} \sum_{i=1}^{N} \left[s_i + \sum_{j_i=1}^{s_i} c_{j_i} - p_{\mathrm{cr}}(p^+) \sum_{j_i=1}^{s_i} (1 - \delta_{c_i,0}) \right].
\end{aligned} \tag{10}
$$

The detailed derivation of Eq. (10) can be found in the Appendix B. Finally, if we define $M_{(1)}^+ = \frac{1}{N} \sum_{i=1}^{N} [s_i + \sum_{j_i=1}^{s_i} c_{j_i}]$, $S = \frac{1}{N} \sum_{i=1}^{N} s_i$, and $\langle 1 - \delta_{c_i,0} \rangle = \frac{1}{s_j} \sum_{j_i=1}^{s_i} (1 - \delta_{c_{j_i},0})$ (see Appendix B), then we can rewrite the condition (6) for microtubule amplification as

$$
M = [p^+ + (1 - p^+) R_d^-(d)] \\
\times \left[M_{(1)}^+ - p_{\mathrm{cr}}(p^+) S \frac{1}{N} \sum_{i=1}^{N} \langle 1 - \delta_{c_i,0} \rangle \right] > 1. \tag{11}
$$

The resolution of the equation associated to this inequality provides the critical threshold for the probability of stabilization-after-severing $p_{\mathrm{crit},(2)}^+$ in order to have amplification. We refer to this approximation as *two-crossovers* approximation. The expression (11) contains two quantities, $M_{(1)}^+$ and S, that cannot be analytically calculated but can be easily measured with computer simulations. On the other hand, in the following sections we are going to analytically calculate the terms $p_{\mathrm{cr}}(p^+)$ and $\frac{1}{N} \sum_{i=1}^{N} \langle 1 - \delta_{c_i,0} \rangle$. In this way, we
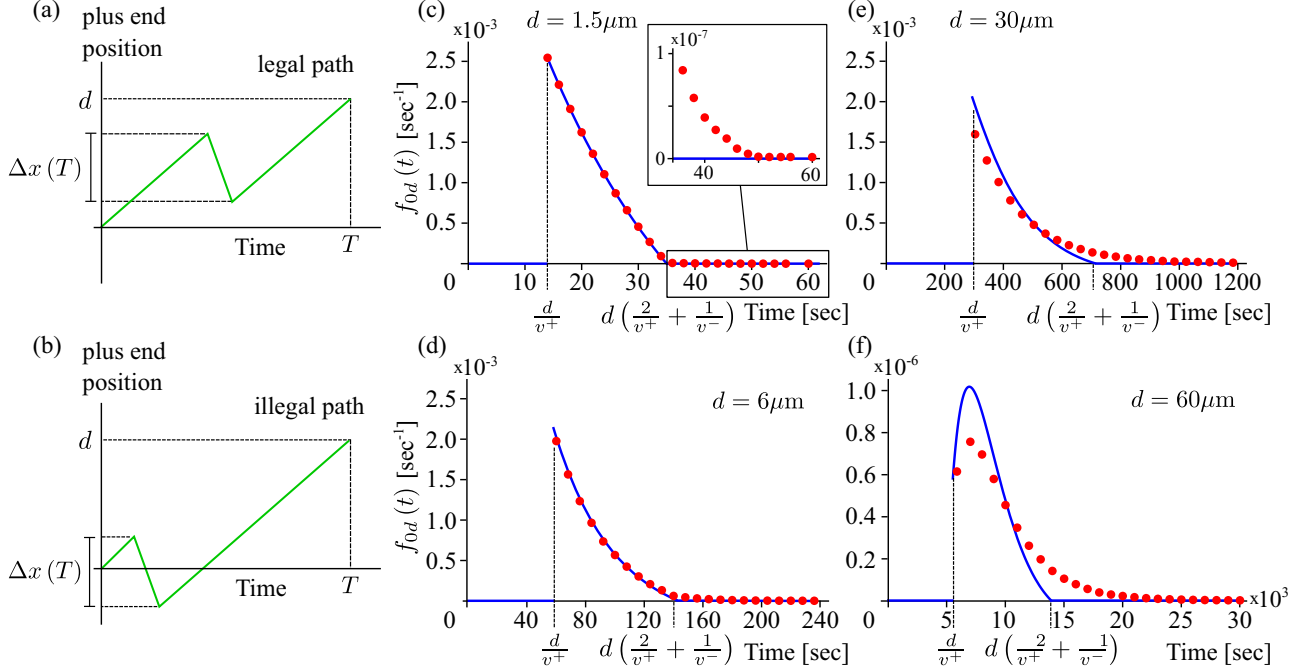
FIG. 4. (a) Legal and (b) illegal path for a microtubule to reach the target at a distance d in a first-passage time T. Only one catastrophe and one rescue are allowed. [(c)–(f)] Comparison between simulations (red dots) and theory (blue line) for the nondirect part $f_d(t)$ of the first-passage time distribution. [(b) and (c)] Our theory nicely fits simulations for relatively close targets ($d = 1.5\,\mu$m, $d = 6\,\mu$m), [(d) and (e)] while it is not very good for more distant targets ($d = 30\,\mu$m, $d = 60\,\mu$m).

will make a better prediction off the critical probability of stabilization-after-severing in order to have amplification.

C. Analytical approach

In this section we are going to calculate the critical probability of stabilization-after-severing. To that end, we first need to calculate $p_{cr}(p^+)$ and $\frac{1}{N}\sum_{i=1}^{N}\langle 1 - \delta_{c_i,0}\rangle$. In order to do so, and because of the complexity of the model, we make the approximation that the entire grid of transverse microtubules is replaced by just two transverse microtubules. This reduces the total number of possible crossovers to two. Therefore, we first calculate the FPTD for a longitudinal microtubule to create a crossover with a transverse, as we will need it for the formulation of our *two-crossovers approximation*. Then, we give some analytical results of the one-crossover approximation already introduced in the previous section. Finally, we present the two-crossovers approximation and we show that we can use it to calculate the critical probability of stabilization-after-severing with a good degree of accuracy.

1. The first-passage time distribution

The creation of new crossovers for a microtubule undergoing dynamic instability is intimately linked to a FPTD problem for the same microtubule to reach a target. Here we face this problem by making use of an approach where we consider all possible legal paths to reach the target, given the knowledge of the time needed to reach it.

The first-passage time problem for a microtubule to reach length x_1 starting from x_0 in the absence of severing can be seen as a reverse lifetime problem, in the sense that in place of studying the reaching of the target at x_1 we study the

survival of the microtubule until it arrives at x_1, as if it is shrinking from x_0 to x_1. In this way, the growing speed of the microtubule acts as its shrinking speed, its catastrophe rate as the rescue rate, and vice versa. However, with this approach we assume that a microtubule "shrinking" from x_0 can undergo a "rescue" and grow beyond the initial position x_0. This means that the microtubule assumes negative length. To avoid this, we need to take into account only the paths from x_0 to x_1 that never shrink below x_0. Hence, if $L_\sigma(t|x_1 - x_0)$ is the lifetime distribution for microtubules with initial length $x_1 - x_0$ and initial state σ (see Appendix A), then we define

$$L_\sigma^{\text{target}}(t, x_1 - x_0) = L_\sigma(t|x_1 - x_0)|_{\substack{v^\pm \to v^\mp, \\ r_c \leftrightarrow r_r}}, \qquad (12)$$

as the FPTD to reach the target, including the possibility of assuming negative length. Therefore, this function must be rescaled by the number of *legal paths* $\Gamma_{x_0 \to x_1}(t)$ that reach the target x_1 at time t, without ever shrinking back to $x < x_0$, calculated over all possible paths that arrive at x_1 at time t, see Figs. 4(a) and 4(b).

For our purpose, the target to reach is a transverse microtubule for the creation of a new crossover, the position of which is at distance d from the starting point, i.e., the previous transverse microtubule. Typically, for the range of values of Table I, every plus end that impinges on a transverse microtubule starting from the previous one either it does so without undergoing any catastrophe or it undergoes one catastrophe and a subsequent rescue. For the dynamic parameters we are considering, the occurrence of multiple catastrophe-rescue events is very unlikely. Indeed, once a microtubule undergoes a catastrophe, the probability of reaching

the target after a single subsequent rescue can be roughly estimated as $(1 - e^{-r_r d/v^-})e^{-r_c d/v^+} \simeq 0.08$, where $p = e^{-r_c d/v^+}$ is the probability of reaching the target without any catastrophe [16]. On the other hand, the occurrence of a second catastrophe-rescue event pair can be roughly estimated as $(1 - e^{-r_c d/v^+})(1 - e^{-r_r d/v^-})^2 e^{-r_c d/v^+} \simeq 0.002$. Therefore we assume that all paths are either direct - no catastrophes, or indirect - one catastrophe and one rescue.

Given the constant growing and shrinking speeds, the amount of time that a microtubule needs to reach the target at d is given by the time needed to reach it in absence of any catastrophe, added to the time spent from a catastrophe to the moment when the original length before the catastrophe is restored. Mathematically, if T_d is the first-passage time and $\Delta x(T_d)$ is the distance walked by the plus end from the catastrophe to the subsequent rescue, then the equation

$$T_d = \frac{d}{v^+} + \Delta x(T_d)\left(\frac{1}{v^+} + \frac{1}{v^+}\right), \quad (13)$$

holds. From Eq. (13) we can find the expression for $\Delta x(T) = \frac{v^+ v^-}{v^+ + v^-}(T - \frac{d}{v^+})$.

Since catastrophes are modelled as Poisson events, if a catastrophe occurs, the probability that it occurs does not depend on the distance from the target. Therefore, the fraction of legal paths can be written as $\Gamma_{0 \to d}(T) = 1 - \frac{\Delta x(T)}{d}$, and, finally, the FPTD as

$$F_{0d}(t) = L_\sigma^{\text{target}}(t, d)\Gamma_{0 \to d}(t)\Theta\left[d\left(\frac{2}{v^+} + \frac{1}{v^-}\right) - t\right], \quad (14)$$

where the Heaviside θ is imposed to allow at most one catastrophe-rescue event.

In order to separate direct paths from indirect paths, it is convenient to split $F_{0d}(t)$ in two parts, and rewrite it as

$$F_{0d}(t) = \delta\left(t - \frac{d}{v^+}\right)e^{-r_c t} + f_{0d}(t), \quad (15)$$

where the term multiplied by the delta function accounts for direct paths, while $f_{0d}(t)$ accounts for indirect paths. From Appendix A that microtubules reach the target with probability $R_d^+(x)$. Therefore $F_{0d}(t)$ is normalized to $R_d^+(x)$ and, as a consequence, the relation

$$\int_0^\infty dt \, f_{0d}(t) = R_d^+(0) - e^{-\frac{r_c d}{v^+}} \quad (16)$$

holds.

We run $N = 10^6$ simulations of microtubules undergoing dynamic instability in a strip of width d, and we create the histogram of the arrival times for the microtubules that reach the target with an indirect path. These simulations are independent from those performed in Sec. III A and Sec. III B. Indeed, here we only keep track of the time needed by single microtubules to reach a target at distance d, and no severing events are involved. Figures 4(c) and 4(d) shows that the approximation of only one catastrophe-rescue event is a good approximation when the target is relatively close compared to the dynamic parameters of the microtubules, while it apparently fails when the target is more distant, see Figs. 4(e) and 4(f). However, it is convenient to point out that, for $d \gg \bar{l}$, we observe a very few arrivals at the target, since

from Eq. (A1) we notice that the arrival probability $R_d^+(0)$ decays as $e^{-d/\bar{l}}$. On the other hand, in the unbounded-growth regime, since a fraction $1 - \frac{r_c v^-}{r_r v^+}$ of the microtubules always arrives at the target, for distant targets the approximation of one catastrophe-rescue event is no longer accurate.

2. One-crossover theory

Naïvely, one can think that once a crossover is created, the probability $p_{\text{sev}}^{(1)}$ of resolving it with a severing event is given by the competition between two independent events: microtubule lifetime, expressed by the random variable $T_+(x)$ with density function given by Eq. (A5), and severing waiting time at the crossover, with random variable τ_d and density function defined in Eq. (1). Then, if we define the random variable $t = \tau_d - T_0$, we can calculate its probability density function by using the relation $P_z(z = x + y) = \int_{-\infty}^{+\infty} dz' P_x(z - z')P_y(z')$, where P_i is the probability density function of the random variable $i = x, y, z$, and x and y are independent random variables. In our case, the probability density function is

$$P_{\tau_d - T_+(0)}(t) = \int_{-\infty}^{+\infty} dt' \, W_{k,\theta}(t + t')L_+(t'|0). \quad (17)$$

Hence, the probability that the event "severing" happens before the event "return" is $\mathbb{P}[t < 0] = \int_{-\infty}^0 dt \, P_{\tau_d - T_+(0)}(t)$. This probability is not yet the probability of resolving a crossover with a severing event: Indeed, microtubules in the unbounded-growth regime have a finite probability of growing indefinitely. For those, the lifetime $T_+(0) \to \infty$ is infinite. Therefore, the probability of resolving a crossover with a severing event is

$$p_{\text{sev}}^{(1)} = S_+(\infty|0) + [1 - S_+(\infty|0)]\int_{-\infty}^0 dt \, P_{\tau_0 - T_+(0)}(t), \quad (18)$$

where $S_+(\infty|0)$ is the ultimate survival probability defined in the Appendix A. As a consequence the probability of resolving a crossover with a shrinkage is

$$p_{\text{shrink}}^{(1)} = 1 - p_{\text{sev}}^{(1)}. \quad (19)$$

However, with this approach we neglect the number of crossovers removed by shrinkage after the severing at a second crossover and, therefore, the dependency on p^+. In other words, the one-crossover theory does not take into account that some microtubules that would have been severed at d are not anymore severed there because an eventual severing at nd, $n > 1$, can in principle shorten their lifetimes and make them shrink below d, resulting in the resolution of the crossover by a shrinkage induced by the severing at nd, see Fig. 5.

3. Two-crossovers theory

In order to take into account the influence of a crossover on the resolution of the previous one, we calculate the probability of resolving a crossover with a severing event in a scenario in which we have two transverse microtubules, at position d and $2d$, respectively. We make the further approximation that a microtubule cannot be severed two times at the same crossover. We denote the probability of having a severing event at d with $p_{\text{sev}}^{(2)}$ and, consequently, the probability of resolving a crossover with shrinkage with $p_{\text{shrink}}^{(2)} = 1 - p_{\text{sev}}^{(2)}$.
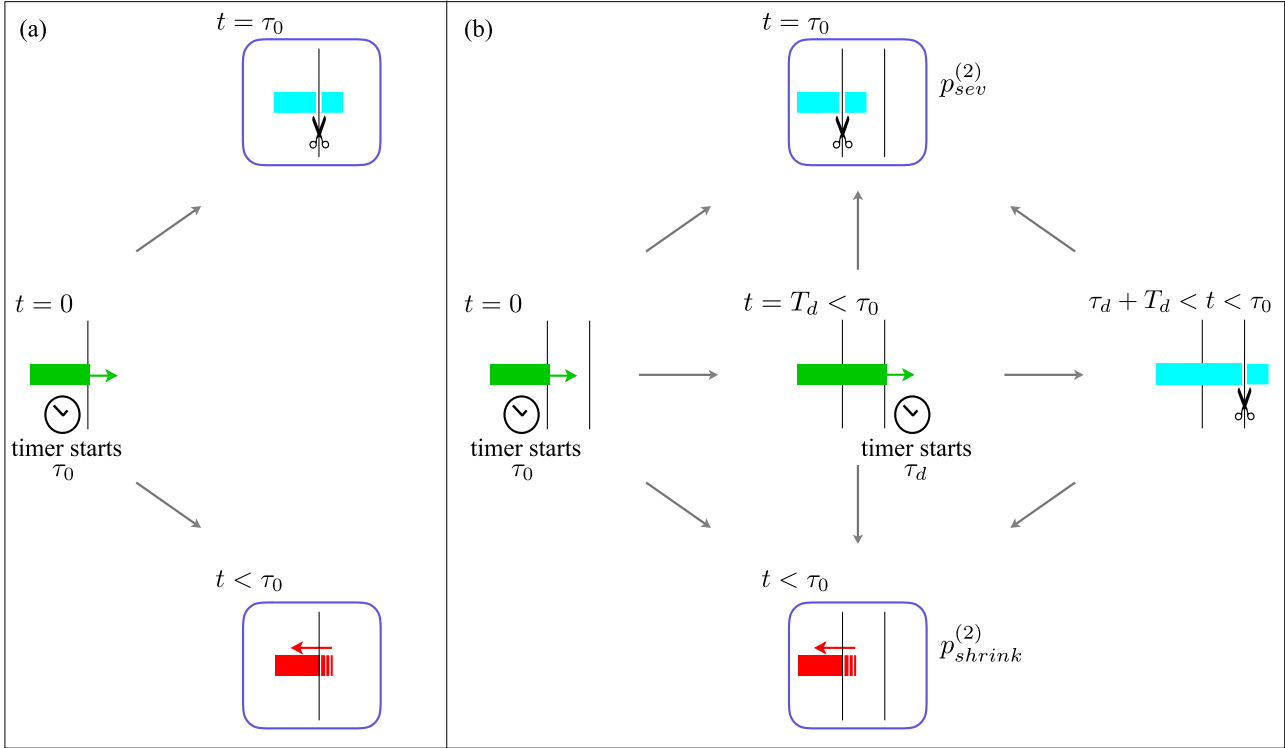
FIG. 5. Schematic of the full one-crossover theory (a). The newly created crossover can be resolved either by the shrinkage of the plus end below the crossover itself (lower blue square) or by the severing at crossover (upper blue square). Schematic of the full two-crossovers theory (b). The first crossover created can be resolved either by the shrinkage of the longitudinal microtubule with probability $p_{shrink}^{(2)}$ (sum of all paths that bring to the lower blue square) or by the severing at crossover with probability $p_{sev}^{(2)}$ (sum of all paths that bring to the upper blue square). Whether the severing at the first crossover occurs or not also depends on what happens at the second crossover: A severing event at the second crossover alters the dynamic instability of the lagging microtubule, and hence its probability of shrinking before being severed at the first crossover.

Figure 5(b) shows the three distinct ways in which the newly created crossover at d can be resolved by shrinkage or severing: (1) The microtubule shrinks (is severed) without reaching $2d$, (2) the microtubule shrinks (is severed) after reaching $2d$ but without being severed there, and (3) the microtubule shrinks (is severed) after reaching $2d$ and after being severed there. The third case bears a dependency on p^+.

We first notice that $p_{shrink}^{(2)}$ can be split in two probabilities, i.e., $p_{shrink}^{(2)} = q_{sev} + q_{shrink}$, where q_{sev} is the probability of shrinkage after severing at $2d$ [path $\longrightarrow \longrightarrow \nearrow$ of Fig. 5(b)], while q_{shrink} is the probability of shrinkage without any severing [paths $\longrightarrow \downarrow$ or $\searrow$ of Fig. 5(b)]. Furthermore, since q_{sev} depends on the dynamic behavior of the microtubule just after the severing event, it carries a dependency on p^+ and can be split again in $q_{sev}(p^+) = p^+ q_{sev,+} + (1 - p^+)q_{sev,-}$, where $q_{sev,\sigma}$ is the probability of shrinkage after being severed at $2d$ with the newly created plus end in the state σ. The derivation of $q_{sev,\sigma}$ can be found in Appendix C.

As regards the probability q_{shrink} that microtubules shrink below d without being severed there, we observe that such a probability accounts all cases in which crossovers are resolved by shrinkage in absence of the crossover at $2d$, i.e., $p_{shrink}^{(1)}$, except for those cases in which microtubules that in principle would have shrunk back, do not have enough time to do so because they are severed at $2d$. We denote this probability with q_{ns}, and hence $q_{shrink} = p_{shrink}^{(1)} - q_{ns}$. The derivation of q_{ns} can be found in Appendix C.

Therefore, the final expressions for the probabilities of resolving a crossover with a severing and with a shrinkage are

$$p_{shrink}^{(2)}(p^+) = p_{shrink}^{(1)} - q_{ns} + q_{sev}(p^+), \qquad (20)$$

$$p_{sev}^{(2)}(p^+) = p_{sev}^{(1)} + q_{ns} - q_{sev}(p^+). \qquad (21)$$

Note that $q_{sev}(p^+)$ can be rewritten as

$$q_{sev}(p^+) = q_{sev,-} - (q_{sev,-} - q_{sev,+})p^+,$$

where the term in the braces is always positive. Indeed, since a microtubule initially in the growing state takes more time to completely depolymerize than a microtubule in the shrinking state, its probability of resolving the crossover at d before being severed there is smaller than in the opposite case. Consequently, from Eq. (21) the probability $p_{sev}^{(2)}(p^+)$ of resolving a crossover with a severing event grows linearly with p^+.

By making use of this two-crossovers theory, we finally give a new estimate of the critical probability of stabilization-after-severing by calculating the probabilities $p_{cr}(p^+)$ and $\frac{1}{N}\sum_{i=1}^{N}\langle 1 - \delta_{c_i,0}\rangle$ of Eq. (11). In order to do that, we first define p_{2d} as the probability to have a severing event at $2d$ before an eventual severing event at d. The derivation of p_{2d} can be found in the Appendix C.

We now define the three events A, B, and C as

$$A = \text{shrinkage of microtubule below } d \text{ after severing at } 2d,$$

$$B = \text{severing event at } 2d \text{ before an eventual severing event at } d,$$

$$C = \text{severing event at either } d \text{ or } 2d.$$

The three events are nested as $A \subset B \subset C$, and their probabilities are $\mathbb{P}(A) = q_{\text{sev}}(p^+)$, $\mathbb{P}(B) = p_{2d}$, and $\mathbb{P}(C) = p_{\text{sev}}^{(2)}(p^+) - q_{\text{sev}}(p^+) + p_{2d} = p_{\text{sev}}^{(1)} - q_{\text{ns}} + p_{2d}$. Thus, it holds

$$p_{\text{cr}}(p^+) = \mathbb{P}(A|B) = \frac{\mathbb{P}(A \cap B)}{\mathbb{P}(B)} = \frac{\mathbb{P}(A)}{\mathbb{P}(B)} = \frac{q_{\text{sev}}(p^+)}{p_{2d}} \tag{22}$$

and

$$\frac{1}{N}\sum_{i=1}^{N}\langle 1 - \delta_{c_i,0}\rangle = \mathbb{P}(B|C) = \frac{\mathbb{P}(B \cap C)}{\mathbb{P}(C)} = \frac{\mathbb{P}(B)}{\mathbb{P}(C)} = \frac{p_{2d}}{p_{\text{sev}}^{(1)} - q_{\text{ns}} + p_{2d}}. \tag{23}$$

Plugging p_{cr} and $\frac{1}{N}\sum_{i=1}^{N}\langle 1 - \delta_{c_i,0}\rangle$ into the equality associated to inequality (11), we finally calculate the critical threshold for the probability of stabilization-after-severing $p_{\text{crit},(2)}^+$, that is,

$$p_{\text{crit},(2)}^+ = \frac{1}{2S\Delta q_{\text{sev}}\beta[1 - R_d^-(d)]}\Big\{(M_0^+ - S\alpha\beta)[1 - R_d^-(d)] - S\Delta q_{\text{sev}}\beta R_d^-(d)$$

$$+ \sqrt{[(M_0^+ - S\alpha\beta)(1 - R_d^-(d)) + S\Delta q_{\text{sev}}\beta R_d^-(d)]^2 - 4S\Delta q_{\text{sev}}\beta[1 - R_d^-(d)]}\Big\}, \tag{24}$$

where

$$\alpha = p_{\text{sev}}^{(1)} + q_{\text{ns}} - q_{\text{sev},-},$$

$$\beta = \frac{1}{p_{\text{sev}}^{(1)} - q_{\text{ns}} + p_{2d}},$$

$$\Delta q_{\text{sev}} = q_{\text{sev},-} - q_{\text{sev},+}.$$

Table II shows a very good agreement between our predicted critical probability of stabilization-after-severing in the two-crossovers approximation and the critical probability obtained with our simulations in the whole grid of transverse microtubules for different choices of dynamic parameters, confirming our hypothesis that, in order to study the critical properties of the system, we can approximate the entire grid of transverse microtubules with just two of them without any considerable loss of accuracy.

IV. DISCUSSION

Our aim was to obtain a deeper insight into the conditions under which templated severing of microtubules at microtubule crossovers can lead to exponential proliferation of a new population of microtubules, as observed in the recent experiments on the light-induced reorientation of the plant microtubule cortical array. To that end we separately considered the role of the microtubule growth state, be it bounded or unbounded, and that of the stabilization-after-severing effect previously identified as a key component of the amplification process. Simulations revealed a striking difference between the unbounded and the bounded microtubule growth regimes. In the unbounded-growth regime, which appears to be salient for the experimental situation, amplification due to templated severing will occur even in the absence of stabilization-after-severing. The reason is that in this growth regime

microtubules in principle have infinite lifetime, allowing them (and their descendants after severing) to be severed without limit, which by itself is sufficient to drive the amplification. There still is a role for the probability of stabilization-after-severing, but only as a moderator for rate of amplification and the probability of success per microtubule. In contrast, in the bounded-growth regime an microtubule can in principle only be severed a finite number of times. In this case amplification can only occur if the process is biased by a sufficiently high probability of stabilization-after-severing. When the system is below a critical value of this parameter, a newly nucleated microtubule, and all of its descendants through severing, is sure to go extinct. The value of this critical stabilization-after-severing probability depends strongly on the probability of a newly severed microtubule to cross the interval between neighboring transverse microtubules, so that it can be severed in turn, a crucial step in the amplification process. This prompted us to develop a—to the best of our knowledge—novel approach to calculating the appropriate first-passage time distribution, using an approach that may find application in other stochastic systems as well. This formed the basis of approximate calculation of the critical stabilization-after-severing probability, which compares favorably with the results obtained from simulations.

Experiments to date have only observed severing-induced amplification in the *Arabidopsis thaliana* hypocotyl system, where microtubules appear to be in the unbounded-growth regime. Unfortunately, therefore, a direct observation of the critical behavior of the amplification probability in response to the change of p^+, here predicted to occur in the bounded-growth regime, is lacking. Moreover, the complex expression (24) for our theoretical prediction for the critical probability of stabilization-after-severing did not allow us to readily identify a single parameter, tuneable either theoretically or

experimentally, in order to systematically vary $p_{\text{crit},(2)}^+$. However, bounded-growing microtubules can, in principle, be created through inducible expression of MAPs aimed at changing the stability of microtubules by, e.g., decreasing the growth speed or by increasing the catastrophe rate. In that case, two options could be envisaged to test the existence of a critical threshold for the probability of stabilization-after-severing in order to observe amplification: (i) suppressing the activity of CLASP and, therefore, reducing the probability of stabilization-after-severing or (ii) reducing the severing rate by modulating katanin activity.

While our work sheds light on the initial phase of the amplification process, understanding the later stages and the stability of the final state remains a challenging problem. Here we have neglected a number of important effects. First, the transverse microtubules were taken to be inert, while in reality they are also dynamic and will tend to be broken down over time as more and more of the available tubulin is incorporated into the exponentially growing population of longitudinal microtubules. This will remove opportunities for severing, and therefore tend to dampen the amplification again. Moreover, as the amplification process develops, the availability of free tubulin dimers, which surely are a limited resource in the cell, is also bound to decrease, which in turn affects both the growth dynamics and nucleation rate. Given our results here, the first effect, depression of the growth speed, could in fact switch the microtubules from the unbounded to the bounded-growth regime, which likely decelerates the amplification process. We are currently exploring these issues, which will be the subject of a follow-up paper.

APPENDIX A: MAIN FEATURES OF THE DOGTEROM-LEIBLER MODEL

1. Splitting probabilities in the interstitial strip

If a microtubule plus end impinges on a transverse microtubule, then it creates a crossover. After the creation of the crossover the plus end is located at $x \in (nd, (n+1)d)$, and, as long as this condition is fulfilled, the dynamics of

microtubules is described by the Dogterom-Leibler model for microtubules with their minus end at nd, regardless the occurrence of a severing event. Without any loss of generality, we can set $n = 0$ and length $l = x$.

Due to the dynamic instability of the plus end, the microtubule either reaches length $x = d$ or shrinks back to length $x = 0$. The occurrence probability of either of these events is described by the so-called *splitting probabilities* $R_0^\sigma(x)$ and $R_d^\sigma(x)$, which describe the probability that a microtubule with initial state σ and initial length x arrives first at length 0 or d respectively. Conservation of probability implies that $R_0^\sigma(x) + R_d^\sigma(x) = 1$.

It is possible to show [16] that

$$R_d^+(x) = \frac{e^{x/\bar{l}} - \frac{r_r v^+}{r_c v^-}}{e^{d/\bar{l}} - \frac{r_r v^+}{r_c v^-}}, \tag{A1}$$

$$R_d^-(x) = \frac{\frac{r_r v^+}{r_c v^-}(e^{x/\bar{l}} - 1)}{e^{d/\bar{l}} - \frac{r_r v^+}{r_c v^-}}, \tag{A2}$$

$$R_0^+(x) = \frac{e^{d/\bar{l}} - e^{x/\bar{l}}}{e^{d/\bar{l}} - \frac{r_r v^+}{r_c v^-}}, \tag{A3}$$

and

$$R_0^-(x) = \frac{e^{d/\bar{l}} - \frac{r_r v^+}{r_c v^-}e^{x/\bar{l}}}{e^{d/\bar{l}} - \frac{r_r v^+}{r_c v^-}}. \tag{A4}$$

Interestingly, these expressions hold for both bounded and unbounded-growth case. This is a direct consequence of the fact that in a strip both regimes produce a steady-state solution [14].

2. Microtubule lifetime and survival probability

The lifetime density function $L_\sigma(t|x)$ of a microtubule with initial length x and initial state σ, is defined as the distribution of the time needed by microtubules to completely depolymerize.

In the bounded-growth regime all microtubules have a finite lifetime, hence $L_\sigma(t|x)$ is normalized to 1. However, in the unbounded-growth a fraction of microtubules grows linearly in time. It follows that for unbounded-growth microtubules, the lifetime density function can be defined only for the fraction of microtubules the lifetime of which is finite.

In the bounded-growth regime, the lifetime density functions are [17]

$$L_+(t|x) = \Theta\left(t - \frac{x}{v^-}\right)\frac{r_c}{v^+t + x}e^{-[r_r(v^+t+x)+r_c(v^-t-x)]}\left\{x\,I_0\left[\frac{2}{v^+ + v^-}\sqrt{r_r r_c(v^+t+x)(v^-t-x)}\right]\right.$$

$$\left. + \frac{v^+}{r_c}\sqrt{\frac{r_c(v^-t-x)}{r_r(v^+t+x)}}I_1\left[\frac{2}{v^+ + v^-}\sqrt{r_r r_c(v^+t+x)(v^-t-x)}\right]\right\}, \tag{A5}$$

$$L_-(t|x) = \delta\left(t - \frac{x}{v^-}\right)e^{-r_r t} + \Theta\left(t - \frac{x}{v^-}\right)\sqrt{\frac{r_c r_r}{(v^+t+x)(v^-t-x)}}x$$

$$\times e^{-[r_r(v^+t+x)+r_c(v^-t-x)]}I_1\left[\frac{2}{v^+ + v^-}\sqrt{r_r r_c(v^+t+x)(v^-t-x)}\right], \tag{A6}$$

where $I_0(\cdot)$ and $I_1(\cdot)$ are the modified Bessel functions of order 0 and 1, respectively.

In order to obtain the densities in the unbounded-growth regime, we need to by divide Eq. (A5) and Eq. (A6) by $1 - S_+(\infty|x)$ and $1 - S_-(\infty|x)$, respectively, where $S_\sigma(\infty|x)$ is the fraction of microtubules with initial length x and initial state σ that never completely depolymerize. Due to their finite lifetime, in the bounded-growth regime these fractions are identically 0. The fractions $S_\sigma(\infty|x)$ are called *ultimate survival probabilities*, and they are

$$S_+(\infty|x) = \begin{cases} 1 - \frac{r_c v^-}{r_r v^+} \exp\left(-\frac{r_r v^+ - r_c v^-}{v^+ v^-}x\right) & \text{if unbounded-growth regime,} \\ 0 & \text{if bounded-growth regime,} \end{cases} \tag{A7}$$

$$S_-(\infty|x) = \begin{cases} 1 - \exp\left(-\frac{r_r v^+ - r_c v^-}{v^+ v^-}x\right) & \text{if unbounded-growth regime,} \\ 0 & \text{if bounded-growth regime.} \end{cases} \tag{A8}$$

APPENDIX B: DERIVATION OF THE SIZE OF THE OFFSPRING OF A MICROTUBULE

Here, we derive the expression for the size of the offspring of a microtubule in the one and two-crossovers approximations.

First, we introduce the one-crossover approximation by removing the dependency on p^+ from the right-hand side of Eq. (8). We assume that $b_{c_{j_i}} = 0$ for every j_i. This implies that, when a severing event occurs at nd, $n > 1$, then all previous crossovers are resolved by a severing event. With this approximation, we replace m_i with

$$m_i^{(1)} = s_i + \sum_{j_i=1}^{s_i} c_{j_i}, \tag{B1}$$

see Fig. 6. Analytically, we cannot calculate neither s_i nor c_{j_i}, but these quantity are easily measurable with computer simulations. We average $m_i^{(1)}$ over $N = 10^5$ simulations to find the first approximation for M^+, i.e., $M_{(1)}^+ = \frac{1}{N}\sum_{i=1}^N m_i^{(1)} = 2.61$. Therefore, from Eq. (7), we can calculate the first estimate of the critical probability of stabilization-after-severing, i.e., $p_{\text{crit},(1)}^+ = 0.316$, against the computationally measured one $p_{\text{crit}}^+ = 0.360$. Table II shows a comparison between $p_{\text{crit},(1)}^+$ and p_{crit}^+ for different sets of dynamic parameters. The table shows that, even though our one-crossover approximation provides a reasonable estimate of the critical probability, we systematically underestimate it.

Now we introduce the two-crossovers approximation by assuming that after a severing at nd, $n > 1$, all crossovers at d, $2d$, $\ldots$, $(n-2)d$ are resolved by a severing event, while the crossover at $(n-1)d$ is resolved by a shrinkage with probability $p_{\text{cr}}(p^+)$ and by a severing with probability $1 - p_{\text{cr}}(p^+)$. Our aim is to give a better estimate of p_{crit}^+ than in the one-crossover approximation. Here

$$b_{c_{j_i}} = \left(1 - \delta_{c_{j_i},0}\right)p_{\text{cr}}(p^+).$$

With this definition for $b_{c_{j_i}}$, we approximate m_i with

$$m_i^{(2)} = s_i + \sum_{j_i=1}^{s_i}\left[c_{j_i} - \left(1 - \delta_{c_{j_i},0}\right)p_{\text{cr}}(p^+)\right]. \tag{B2}$$

From this equation, we can observe that

$$\sum_{j_i=1}^{s_i}\left(1 - \delta_{c_{j_i},0}\right)p_{\text{cr}}(p^+)$$

$$= p_{\text{cr}}(p^+)[s_i - (\delta_{c_1,0} + \delta_{c_2,0} + \cdots + \delta_{c_{s_i},0})]$$

$$= p_{\text{cr}}(p^+)[s_i - s_i\langle\delta_{c_i,0}\rangle]$$

$$= p_{\text{cr}}(p^+)s_i\langle 1 - \delta_{c_i,0}\rangle, \tag{B3}$$

where the average value $\langle\delta_{c_i,0}\rangle$ is calculated over all severing events that a leading microtubule undergoes along its lifetime. Consequently, $\langle 1 - \delta_{c_i,0}\rangle$ is the fraction of severing events
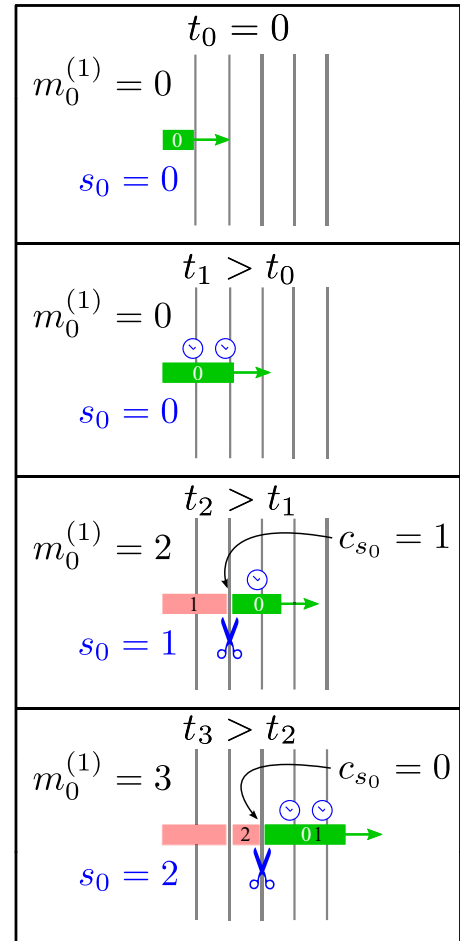
FIG. 6. Schematic of the count of the size of the offspring $m_0^{(1)}$ of a microtubule labeled by 0 created by severing in the growing state. When a crossover is created, the competition severing-shrinking takes place, and if the severing occurs, then the counter for the number of severing events s_0 gains one unity, while the size of the offspring gains $1 + c_{s_0}$. We keep track of the leading microtubule as it can generate other descendants, further increasing $m_0^{(1)}$. We do not keep track of the lagging microtubules created by severing.

that a leading microtubule undergoes at nd with $n > 1$. If we combine Eqs. (B1), (B2), and (B3) together, and we average over N, then we obtain

$$
\begin{aligned}
M_{(2)}^+ &= \frac{1}{N} \sum_{i=1}^{N} m_i^{(2)} \\
&= \frac{1}{N} \sum_{i=1}^{N} \left[s_i + \sum_{j_i=1}^{s_i} c_{j_i} - p_{\text{cr}}(p^+) s_i \langle 1 - \delta_{c_i,0} \rangle \right] \quad \text{(B4)} \\
&= M_{(1)}^+ - p_{\text{cr}}(p^+) S \frac{1}{N} \sum_{i=1}^{N} \langle 1 - \delta_{c_i,0} \rangle,
\end{aligned}
$$

where $S = \frac{1}{N} \sum_{i=1}^{N} s_i$ and where we assumed that the correlation between the number of severing events that occur

along the lifetime of a microtubule and the fraction of them that occur at nd with $n > 1$ is negligible. In this case, if $N \gg 1$, then by the law of large numbers $\frac{1}{N} \sum_{i=1}^{N} \langle 1 - \delta_{c_i,0} \rangle$ is the probability that a microtubule is severed at nd with $n > 1$, sampled over all cases in which a severing event has occurred. By replacing M^+ with $M_{(2)}^+$ in Eq. (6), we obtain the final amplification condition (11). Table II shows that the two-crossovers reproduces the computationally measured critical probability of stabilization-after-severing with a good degree of accuracy.

APPENDIX C: DERIVATION OF SEVERING AND SHRINKAGE PROBABILITIES

In order to calculate $q_{\text{sev},\sigma}$ we first define the following random variables:

$$
\begin{aligned}
\tau_d &= \text{severing waiting time at } d, \\
\tau_{2d} &= \text{severing waiting time at } 2d, \\
T_d &= \text{FPT from the first to the second crossover, i.e., from } d \text{ to } 2d, \quad \text{(C1)} \\
T_\sigma(x) &= \text{lifetime of a microtubule with initial state } \sigma \text{ and initial length } x, \\
\widetilde{\tau}_{2d} &= \text{severing waiting time at } 2d \text{ given that the severing occurs.}
\end{aligned}
$$

τ_d and τ_{2d} have probability density function $W_{k\theta}(t)$ defined in Eq. (1), while the probability density function of T_d is $F_{0d}(t)$ from Eq. (14). The probability density function of $T_\sigma(x)$ is $L_+(t|x)$ defined in the Appendix A. Finally, the probability density function of $\widetilde{\tau}_{2d}$ can be calculated by observing that the event "severing" and the event "shrinkage" are independent. Therefore, the cumulative function $\Phi_{\widetilde{\tau}_{2d}}(t) = \mathbb{P}[\widetilde{\tau}_{2d} < t]$ can be written as

$$
\Phi_{\widetilde{\tau}_{2d}}(t) = \mathbb{P}\{(\tau_{2d} < t) \cap [\tau_{2d} < T_+(0)]\} = \frac{1}{Z_W} \int_0^t dt'\, W_{k,\theta}(t') \int_{t'}^{\infty} dt''\, L_+(t''|0), \quad \text{(C2)}
$$

where

$$
Z_W = \int_0^{\infty} dt\, W_{k,\theta}(t) \int_t^{\infty} dt'\, L_+(t'|0). \quad \text{(C3)}
$$

Thus, the probability density function $\widetilde{W}_{k\theta}(t)$ of $\widetilde{\tau}_{2d}$ is

$$
\widetilde{W}_{k\theta}(t) = \frac{d}{dt} \Phi_{\widetilde{\tau}_{2d}}(t) = \frac{1}{Z_W} W_{k\theta}(t) \int_t^{\infty} dt'\, L_+(t'|0). \quad \text{(C4)}
$$

The probability $q_{\text{sev},\sigma}$ is the probability that a microtubule reaches $2d$, it is severed there with newly created plus end in the state σ, and finally shrinks back below d *before* being severed at d. In $S_+(\infty|0)$ of the cases (i.e., for indefinitely growing microtubules), this event occurs if $T_1 = \tau_d - T_d - \tau_{2d} - T_\sigma(d) > 0$, with probability density function of T_1 defined by

$$
P_{T_1}(t) = \int_{\mathbb{R}^3} dt' dt'' dt'''\, W_{k\theta}(t + t' + t'' + t''') F_{0d}(t') W_{k\theta}(t'') L_\sigma(t'''|d). \quad \text{(C5)}
$$

In the remaining $1 - S_+(\infty|0)$ of the cases (i.e., for microtubules with a finite lifetime), the event occurs if $T_2 = \tau_d - T_d - \widetilde{\tau}_{2d} - T_\sigma(d) > 0$, and if it is severed at $2d$, i.e., if $\tau_d < T_+(0)$. The probability density function of T_2 is

$$
P_{T_2}(t) = \int_{\mathbb{R}^3} dt' dt'' dt'''\, \widetilde{W}_{k\theta}(t + t' + t'' + t''') F_{0d}(t') W_{k\theta}(t'') L_\sigma(t'''|d). \quad \text{(C6)}
$$

Hence, the final expression for $q_{\text{sev},\sigma}$ is

$$
q_{\text{sev},\sigma} = R_d^+(0) \left\{ S_+(\infty|0) \int_0^{\infty} dt\, P_{T_1}(t) + [1 - S_+(\infty|0)] \int_0^{\infty} dt\, P_{\tau_d - T_0}(t) \int_0^{\infty} dt\, P_{T_2}(t) \right\} [1 - S_+(\infty|d)]. \quad \text{(C7)}
$$

To calculate q_{ns} we first define the random variable $\widetilde{T}_+$ as the time that a microtubule initially in the growing state and with plus end in $2d$ needs in order to return in the shrinking state at $2d$, given that no severing event occurs at $2d$. Similarly to the derivation of $\widetilde{W}_{k\theta}(t)$, we can derive the probability density function of $\widetilde{T}_+$, that is,

$$
\widetilde{L}_+(t) = \frac{1}{Z_L} L_+(t|0) \int_0^t dt'\, W_{k,\theta}(t'), \quad \text{(C8)}
$$

with

$$Z_L = \int_0^\infty dt\, L_+(t|0) \int_0^t dt'\, W_{k,\theta}(t').$$ (C9)

Therefore, as q_{ns} is the probability that a microtubule reaches length $2d$ and would return to length d but it cannot because it is severed at $2d$, the two conditions that our random variables have to fulfill are $\tau_{2d} < T_+(0)$ and $\tau_d > T_d + \widetilde{T}_+ + T_-(d)$. The former condition had already been discussed before, while the latter is associated to the probability density function

$$P_{\tau_d - T_d - \widetilde{T}_+ - T_-(d)}(t) = \int_{\mathbb{R}^3} dt' dt'' dt''' \, W_{k\theta}(t + t' + t'' + t''') F_{0d}(t') \widetilde{L}_+(t'') L_-(t'''|d).$$ (C10)

Therefore

$$q_{\text{ns}} = R_{0d}^+[1 - S_+(\infty|0)] \int_{-\infty}^0 dt\, P_{\tau_d - T_+(0)}(t) \int_0^\infty dt\, P_{\tau_d - T_d - \widetilde{T}_+ - T_-(d)}(t).$$ (C11)

Finally, in order to calculate the probability p_{2d} to have a severing event at $2d$ before an eventual severing event at d, we notice that we have two different cases. In the first case, the microtubule reaches length $2d$ and it is severed there before being severed at d, i.e., $\tau_d > T_d + \tau_{2d}$. In the second case, the microtubule reaches $2d$ and it is severed there before being severed at d, i.e., $\tau_d > T_d + \widetilde{\tau}_{2d}$, given that the event "severing" wins the competition against the event "shrinkage" at $2d$, or $\tau_{2d} < T_+(0)$. The probability density functions associated to these conditions are, respectively,

$$P_{\tau_d - T_d - \tau_{2d}}(t) = \int_{\mathbb{R}^2} dt' dt'' \, W_{k\theta}(t + t' + t'') F_{0d}(t') W_{k\theta}(t''),$$ (C12)

$$P_{\tau_d - T_d - \widetilde{\tau}_{2d}}(t) = \int_{\mathbb{R}^2} dt' dt'' \, W_{k\theta}(t + t' + t'') F_{0d}(t') \widetilde{W}_{k\theta}(t''),$$ (C13)

$$P_{\tau_{2d} - T_+(0)}(t) = P_{\tau_d - T_+(0)}(t).$$ (C14)

Then

$$p_{2d} = R_{0d}^+ \left\{ S_+(\infty|0) \int_0^\infty dt\, P_{\tau_d - T_d - \tau_{2d}}(t) + [1 - S_+(\infty|0)] \int_{-\infty}^0 dt\, P_{\tau_{2d} - T_+(0)}(t) \int_0^\infty dt\, P_{\tau_d - T_d - \widetilde{\tau}_{2d}}(t) \right\}.$$ (C15)

[1] B. Alberts, A. Johnson, J. Lewis, M. Raff, K. Roberts, and P. Walter, *Molecular Biology of the Cell* (Garland Science, New York, 2007).

[2] T. Mitchison and M. Kirschner, Dynamic instability of microtubule growth, Nature **312**, 237 (1984).

[3] J. C. Sedbrook, MAPs in plant cells: Delineating microtubule growth dynamics and organization, Curr. Opin. Plant Biol. **7**, 632 (2004).

[4] R. Dixit and R. Cyr, The cortical microtubule array: From dynamics to organization, Plant Cell **16**, 2546 (2004).

[5] J. J. Lindeboom, M. Nakamura, A. Hibbel, K. Shundyak, R. Gutierrez, T. Ketelaar, A. M. C. Emons, B. M. Mulder, V. Kirik, and D. W. Ehrhardt, A mechanism for reorientation of cortical microtubule arrays driven by microtubule severing, Science (NY) **342**, 1245533 (2013).

[6] J. J. Lindeboom, M. Nakamura, M. Saltini, A. Hibbel, A. Walia, T. Ketelaar, A. M. C. Emons, J. C. Sedbrook, V. Kirik, B. M. Mulder, and D. W. Ehrhardt, CLASP stabilization of plus ends created by severing promotes microtubule creation and reorientation, J. Cell Biol. **218**, 190 (2019).

[7] P. T. Tran, R. A. Walker, and E. D. Salmon, A metastable intermediate state of microtubule dynamic instability that differs significantly between plus and minus ends, J. Cell Biol. **138**, 105 (1997).

[8] V. Kirik, U. Herrmann, C. Parupalli, J. C. Sedbrook, D. W. Ehrhardt, and M. Hülskamp, CLASP localizes in two discrete patterns on cortical microtubules and is required for cell morphogenesis and cell division in Arabidopsis, J. Cell Sci. **120**, 4416 (2007).

[9] M. Dogterom and S. Leibler, Physical Aspects of the Growth and Regulation of Microtubule Structures, Phys. Rev. Lett. **70**, 1347 (1993).

[10] M. Nakamura, J. J. Lindeboom, M. Saltini, B. M. Mulder, and D. W. Ehrhardt, SPR2 protects minus ends to promote severing and reorientation of plant cortical microtubule arrays, J. Cell Biol. **217**, 915 (2018).

[11] A. Papoulis and S. U. Pillai, *Probability, Random Variables, and Stochastic Processes* (Tata McGraw-Hill, New York, 2002).

[12] W. O. Hancock, Aging gracefully: A new model of microtubule growth and catastrophe, Biophys. J. **109**, 2449 (2015).

[13] A. Akhmanova, Strengthening microtubules by cuts that heal, Dev. Cell **47**, 400 (2018).

[14] B. S. Govindan and W. B. Spillman, Steady states of a microtubule assembly in a confined geometry, Phys. Rev. E **70**, 032901 (2004).

[15] J. W. Vos, M. Dogterom, and A. M. C. Emons, Microtubules become more dynamic but not shorter during preprophase band formation: A possible "search-and-capture" mechanism for microtubule translocation, Cell Motil. Cytoskel. **57**, 246 (2004).

[16] B. M. Mulder, Microtubules interacting with a boundary: Mean length and mean first-passage times, Phys. Rev. E **86**, 011902 (2012).

[17] D. J. Bicout, Green's functions and first passage time distributions for dynamic instability of microtubules, Phys. Rev. E **56**, 6656 (1997).